good preparation (2/2),
experimental implementation (2/2)
and report (5.5/6)(just a few minor remarks)

universität innsbruck

Acousto-optical effect

Alexander Helbok*, Jakob Höck †, Max Koppelstätter‡

March 19, 2024

Abstract

In this report the working principle and some properties of an acousto-optical modulator (AOM) are examined. In such a device, bragg diffraction of laser light can be tuned by inducing acoustic waves into the crystal. We determined the bragg angle and the insertion loss of the AOM. The quality factor was calculated using two different methods, by varying either power or incident angle. Lastly, the maximum efficiency, dependent on the RF-frequency is measured. We could mostly reproduce the AOM's properties as stated by the manufacturer, the two measured quality factors are consistent with each other, varying the frequency is however the much more accurate method.

*alexander.helbok@student.uibk.ac.at
†jakob.hoeck@student.uibk.ac.at
‡max.koppelstaetter@student.uibk.ac.at

Contents

0 Introduction

Let's explore some applications of an Acoustic-Optical Modulator (AOM). Why is this of importance? On the one hand, AOM's serve as swift switches for lasers, enabling rapid operation. On the other hand, this modulator is capable of generating pulsed laser beams and beams with reduced intensity.
This experiment leverages a fundamental optical effect to achieve these valuable features: Bragg's law. But unlike diffraction on a crystal structure/diffraction grating, where the diffraction properties are fixed to material constants, in an AOM one can tune them. By coupling an electric signal to the crystal (TeO_2) via a piezoelectric transducer one can induce density waves into the crystal, locally changing the refractive index. With the adjustment of the amplitude (peak-to-peak voltage), as well as the frequency of the electric signal, it is possible to tune the diffraction behavior to fit ones needs. A primary objective of the experiment is to ascertain the impact of uncertainties and whether they align with theoretically expected behaviours. These uncertainties may involve angular deviations. Additionally, we analyse the AOM's behaviour across various frequencies.
Following a brief theoretical overview and an explanation of the applied theory, this report will present and discuss the evaluated data.

1 Theory

Light exhibits different phenomena when brought into contact with solid matter (E.g. absorption, scattering, diffraction). In this experiment we will make use of a special kind of diffraction, Bragg diffraction. This played a major role in uncovering the internal structure of crystal, exposing the position of their constituting atoms.

1.1 Bragg condition

When shining light onto a crystal structure, the waves get partially reflected by the different lattice planes. In order to get constructive interference, the path difference between the different reflected light waves has to be an integer multiple of its wavelength λ. This is also known as the Bragg condition and is pictured in Figure 1 on the left.

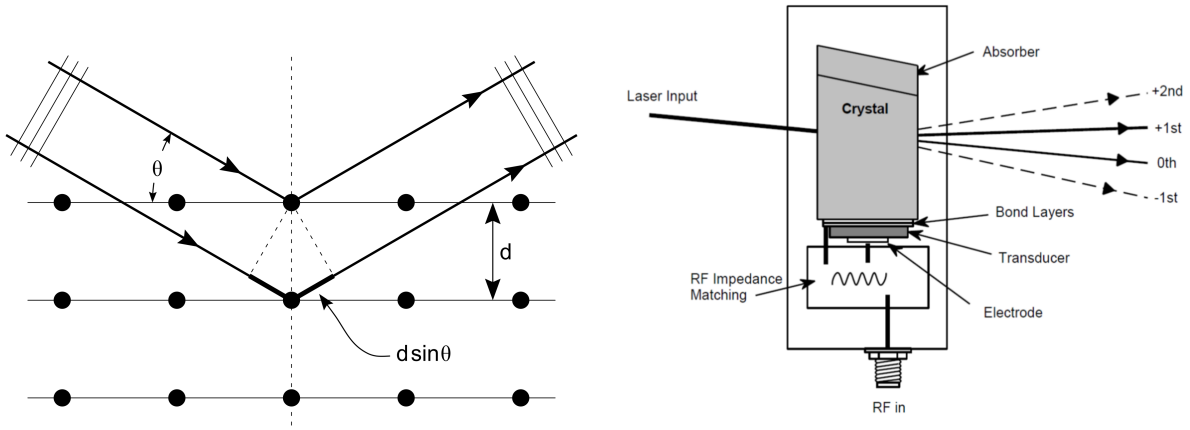

Figure 1: On the left side is the schematic sketch of the Bragg reflection [1]. On the right is an overview of the working principle of an AOM. The RF signal gets coupled to the AOM via a piezo transducer. This creates density modulation inside the crystal, which divert the light beams intensity into higher diffraction orders [2].

Formally, the Bragg condition states that

$$n\lambda = 2d\sin(\theta), \tag{1}$$

where d is the lattice plane spacing, n is an integer and θ is the angle under which the light is shined on the crystal.

1.2 Acousto-optical modules

In Acousto-optical modules (AOM) diffraction does not happen on fixed lattice planes. Instead, a change in refractive index is created by locally changing the density of the material. This can be done by inducing longitudinal waves (sound waves) into one side of the crystal and absorbing them on the other side to suppress standing waves. This creates periodic over- and under densities, which function like the static lattice planes.

The sound waves are created by converting electric signals (from a function generator) into mechanical movement via a piezo element. An overview of an AOM's components is shown in Figure 1 on the right.

As the AOM is not perfectly transparent for light waves, some losses occur due to absorption, which is defined as the ratio between the intensity before and after the AOM

$$IL = 1 - \frac{P_{\text{out}}}{P_{\text{in}}}.$$

Depending on the frequency f_{RF} and the amplitude P_{RF} of the driving signal, more power is moved from the 0^{th} diffraction order (undisturbed transmission) to higher orders. For frequencies around the AOM's resonant frequency $f_0 \sim 80$ MHz [3] most of the power gets diverted into the 1^{st} diffraction order. The efficiency $\varepsilon = P_1/P_{\text{out}}$ is then defined as the ratio between the power in the 1^{st} order and the total power after the AOM.

The efficiency depends on both f_{RF} and P_{RF}. Holding the frequency f_{RF} constant one can derive that

$$\varepsilon \sim \sin^2\left(\frac{\pi}{2}\sqrt{P}\right), \tag{2}$$

with $P = P_{\mathrm{RF}}/P_{\mathrm{sat}}$ the normalized RF power, where P_{sat} describes the saturation power. A change in frequency can also be expressed in a change in bragg angle, which leads to the following relations:

$$\varepsilon \sim \mathrm{sinc}^2\left(\frac{Q}{4}\Delta\right) \quad \text{or} \quad \varepsilon \sim \mathrm{sinc}^2\left(\frac{Q}{4}F\left(1-F\right)\right). \tag{3}$$

Here $\Delta = \delta/\theta_{\mathrm{B}}$ is the normalized angular error and $F = f_{\mathrm{RF}}/f_0$ is the frequency detuning from the resonant point (see [2]).

2 Experimental setup and procedure

Before the actual measuring started, we discussed the safety aspects of working with a laser. Therefore, we dismounted all jewelry and wristwatches to minimize the risk of reflecting the laser in an unwanted direction. After this, we took a look at the mounted optical components and checked if the mirrors were in the correct position, as well as whether the collimation was well-adjusted to get a precise output beam. We used a HeNe Laser with a wavelength of $\lambda = 632.8$ nm. After these steps, we switched off the laser to safely measure the distance between the mirrors and the AOM, as well as the point where we will later measure the distance between the 0^{th} and 1^{st} order diffracted beams. This measurement was taken with a measuring tape with estimated errors of ± 0.2 cm for the first two lengths and ± 0.1 cm for the third length, as we have a very solid measuring point at the end of the beam (actual lengths in Figure 2).

Since we are using an amplifier to increase the signals strength, we have to take the amps gain into consideration when setting the signals amplitude on the frequency generator. From the datasheet (see [4]), we found that the amplifier boosts the signal by 33 dB, which corresponds to an input power increase by a factor of 2000. In order to put 2 W through the AOM (this is the maximum power) we have to set the function generator to 1 mW. This corresponds to a peak-to-peak voltage of 632 mVpp [5]. The frequency generator, where we can adjust these parameters, is shown in Figure 3.

Following this, we initiated the laser and commenced the process of identifying both the 1^{st} and 0^{th} orders of the diffracted beam. The input parameters for the AOM were configured to 500 mW and 80 MHz. With this setup, we accurately determined the Bragg angle by maximizing the power of the 1^{st} order beam by adjusting the rotation mount. Measurements of the mentioned distances were conducted using a measuring tape. The corresponding setup is visually depicted in Figure 2.

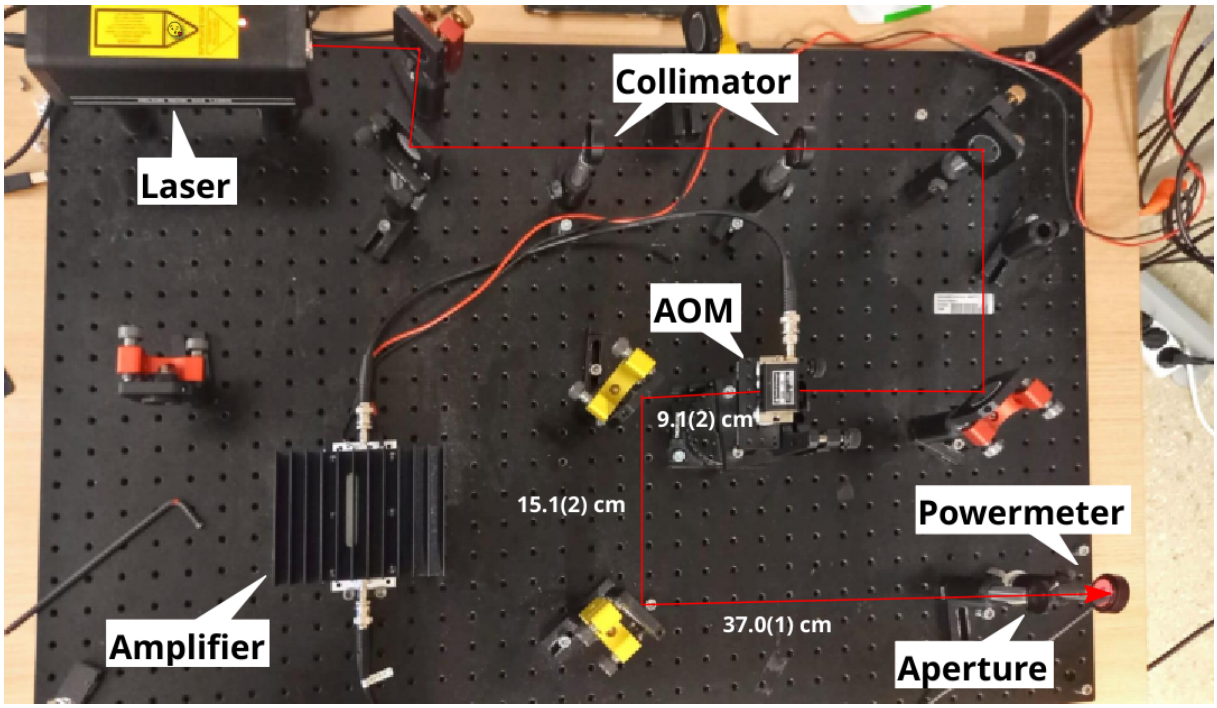

Figure 2: A picture of the experimental setup. The path of the laser beam is traced from the laser in the top left corner to the power meter on the bottom right. All the major components are labeled accordingly. The measured path length from the Acousto-optical Module (AOM) to the power meter is also given.

Afterwards, we measured the power before and after the AOM without a modulation signal to assess the internal losses (IL). Proceeding, the power of the AOM was varied from 0 W to 2 W, with the corresponding mVpp as mentioned above. Opting for 30 mVpp steps, we measured the power of the 0^{th} and the 1^{st} orders to assess ε, thereby positioning ourselves to fit a function referenced in subsection 1.2 to determine the saturation power P_{sat}.

In the next step, the intention was to determine the frequency dependence of the AOM. Therefore, the power was set to 500 mW, and the frequency was modulated in the range of $60-100$ MHz in 3 MHz steps (The last two steps were 2 MHz each to precisely reach 100 MHz). The power of the 1^{st} order was measured, as well as the distance between the 0^{th} and 1^{st} order beam. With this length, we are able to determine the Bragg angle. To obtain a more accurate result, the measurement was taken at a larger distance (by projecting the beams onto a wall). The length after the 2^{nd} mirror after the AOM (37.0(1) cm so far) was extended to 140.0(2) cm.

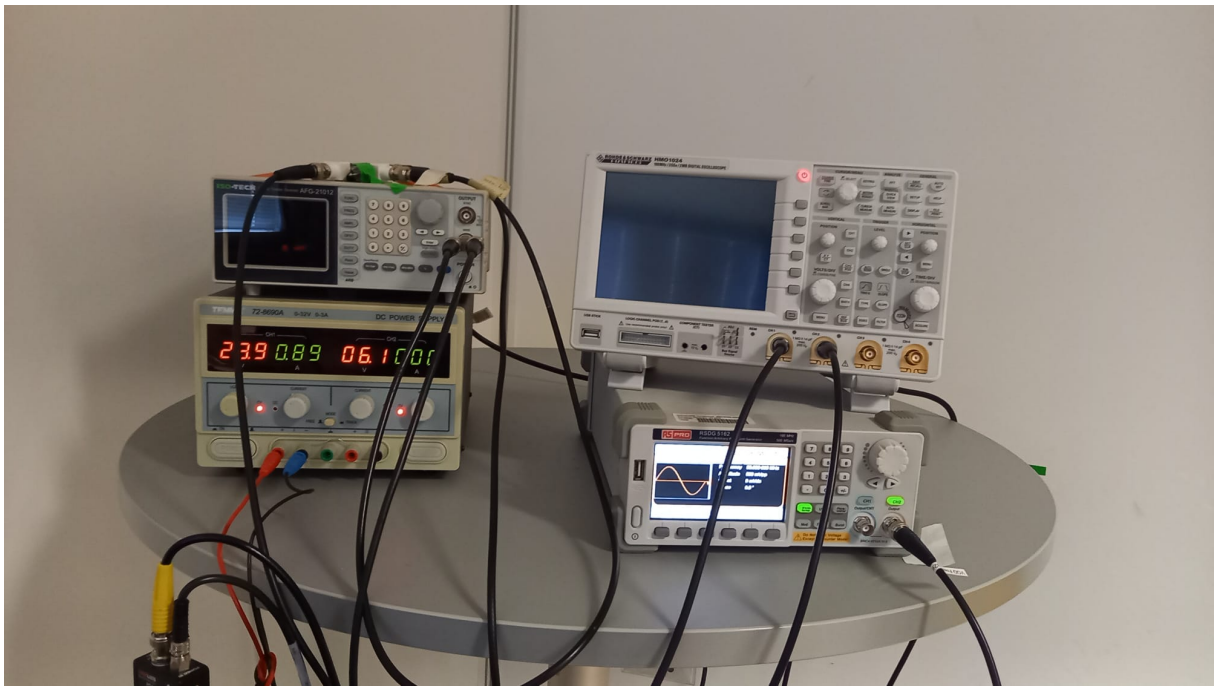

Figure 3: This figure shows a picture of the power supply for the amplifier (on the left) as well as the frequency generator (on the right), where it is possible to set the mVpp and the frequency.

Thereafter, the focus shifted to the angular dependence of the AOM in perspective to the quality factor Q. We began by determining the deadzone of the rotation mount, as well as verifying the gear ratio provided in [6]. For the deadzone, we estimate it to be 5 ticks, and we verified the gear ratio to be 1/25 (25 ticks on the screw are equal to 1°). Now the task was to evaluate the power at the 1^{st} order beam for angles between -1° and 1° with the AOM parameters of 80 MHz and 500 mW. Here we decided to use a step size of 3 ticks in the outer range, and as we got closer to 0°, we made finer steps with 2 ticks. Surprisingly, the maximum value was not at 0°, so we decided to take more values in the positive angular direction to achieve a symmetric measuring range around the maximum value. To minimize measurement errors from the screws deadzone all measurements were made by continuously adjusting the screw from the same direction.

Finally, the task was to analyze the angular dependence of the maximum diffraction efficiency. Therefore, we set the power of the AOM to 500 mW and then changed the frequency in the range of $60 - 100$ MHz, using 5 MHz steps. At each frequency, we aimed to maximize the power of the 1^{st} order by adjusting the angle of the rotation mount and recording the power.

3 Results

In this section, all results of the experiments are presented, including all relevant analysis.

3.1 Measurement of the electronic components and the optimum Bragg angle

Due to geometric considerations, the Bragg angle θ_{B} was calculated as $\theta_{\text{B}} = \arctan(d_{01}/(2d)$, where $d_{01} = 0.8(1)$ cm is the length difference between 0^{th} and 1^{st} order diffracted beams at

the powermeter, and $d = 61.2(3)$ cm is the total path length from the AOM to the powermeter. This results in

$$\theta_B = 6.5(8) \text{ mrad}.$$

The high uncertainty is a direct consequence of the big uncertainty in the measurement of the length difference between zeroth and first diffraction order, which was hard to measure exactly.

In order to determine a exact conversion from the peak-to-peak Voltage in mVpp, which is set at the powermeter, to the RF-power in mW, we use a table given in [5]. We plotted power for the given voltage in the first column of the table, and fitted a quadratic function, as seen in Figure 4. This function type had the best fit quality with a χ_ν well below 1, which when dealing with uncertain measurements indicates that the theory fits the data "too well" (here we have no uncertainty so a small χ_ν is ecpected).

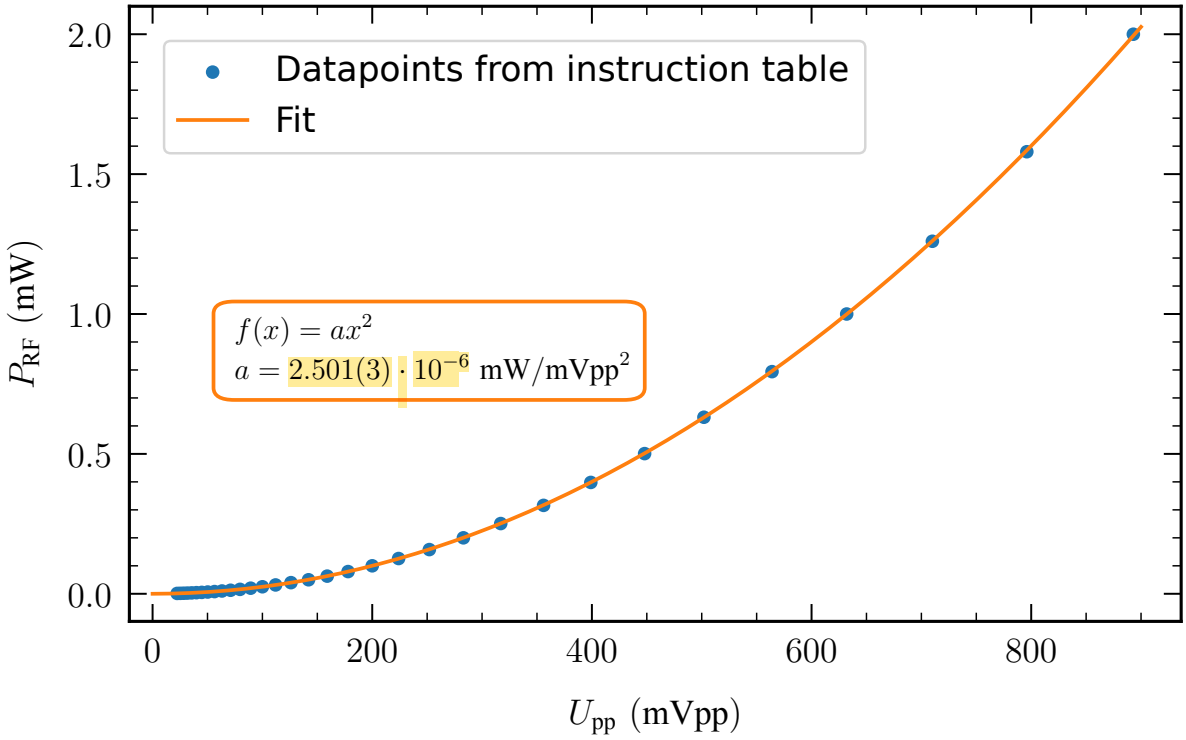

Figure 4: The data points plotted are the given values out of the transformation table in [5]. A quadratic function with given fit parameters helps us transforming values from peak-to-peak-voltage to RF-power.

3.2 Measurement of the intensity dependence and determination of the saturation power

Without applied RF-power, the insertion loss IL was determined using the formula given in subsection 1.2. With $P_{in} = 0.877(5)$ mW and $P_{out} = 0.791(5)$ mW we get

$$IL = 0.098(8).$$

In Figure 5, measured efficiency $\varepsilon = P_i/P_{out}$, with i representing different diffraction orders,

is plotted in dependence of the RF-power. A fit based on Equation (2) is done for the first diffraction order.

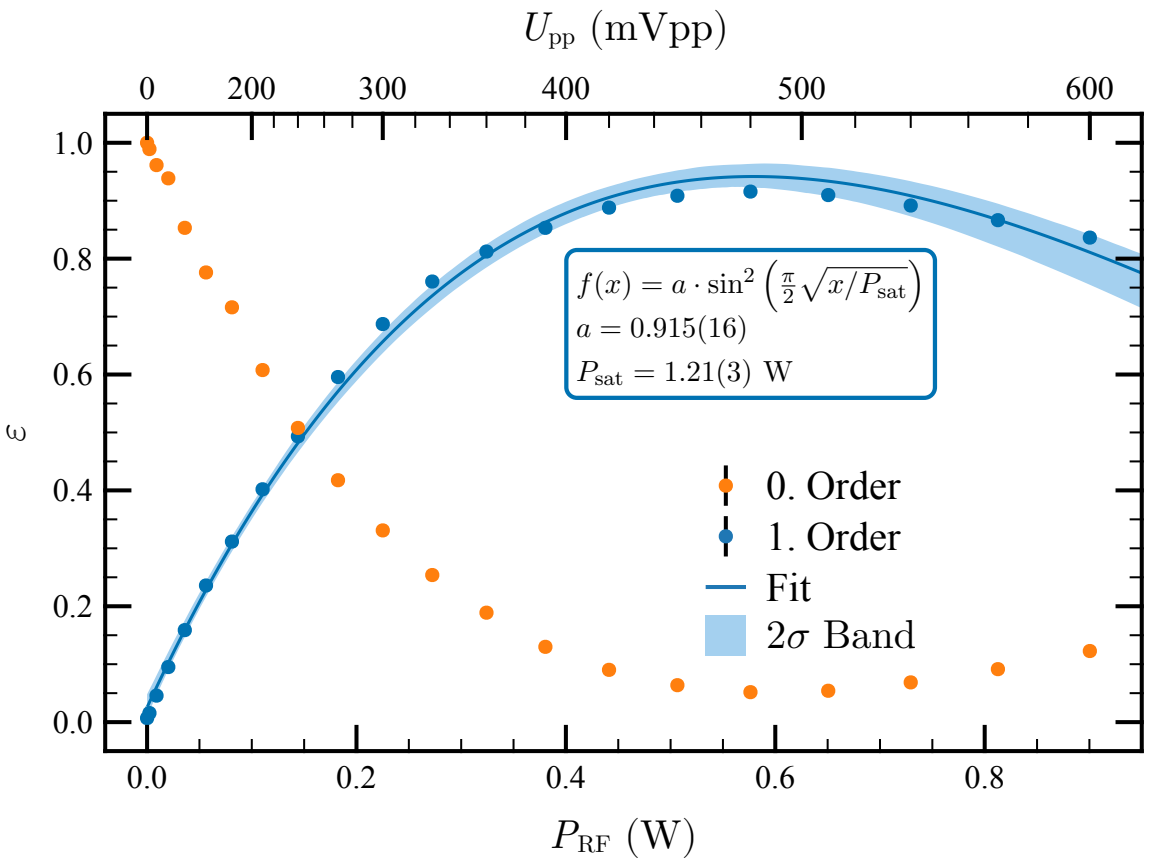

Figure 5: The measured efficiency of the 0^{th} and 1^{st} diffraction orders is shown with varying RF power. On the top x-Axis the values set in the frequency generator are shown, whilst the bottom x-Axis shows the converted power after the amplifier. The errors of the efficiencies are just too small to make out (they are of the order of the dot size). 1^{st} order data was used to fit a $\sin^2$ law, which is shown as blue line with 2σ confidence band.

From this fit, we can extract the saturation power and we get

$$P_{\mathrm{sat}} = 1.21(3)\ \mathrm{W}.$$

3.3 Measurement of the frequency dependence and determination of the quality factor

In Figure 6, the measured efficiency is plotted for varying frequency f_{RF} from 60 MHz to 100 MHz. The uncertainty in frequency is neglected, as we assume it to be much smaller than the uncertainty of the measured power. Thus, its influence can be ignored. In Figure 6 the measured efficiency of the 1^{st} diffraction order is plotted against frequency. From Equation (3) we expect the efficiency to follow a $\sin(x)/x$ relation with regards to frequency. This function has been fitted to the data and can also be seen in Figure 6. The parameters were expressed in a way such as to give them a physical meaning.

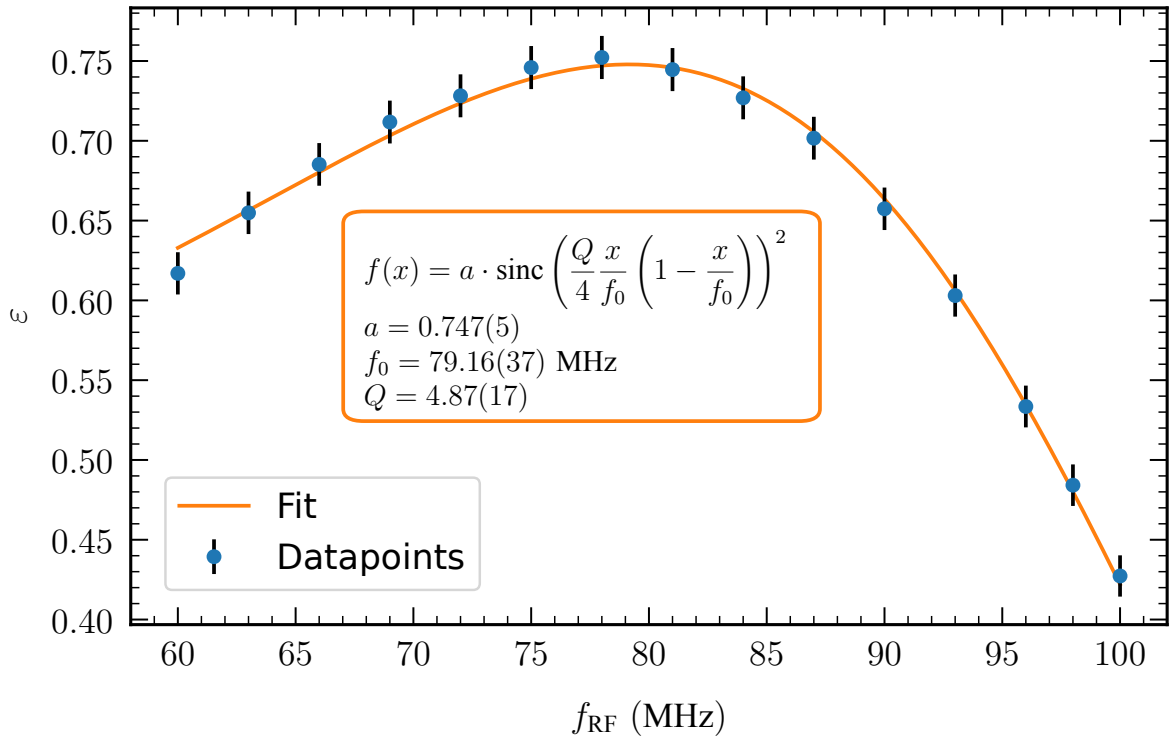

Figure 6: The measured efficiency dependent on frequency is shown. In addition, a fit is given, from which we can deduce a fitted central frequency f_0 and the quality factor Q.

Even though the resonant frequency of the AOM is listed in [1] to be 80 MHz, we chose to include it as a free parameter in the fit, since AOMs can drift in frequency. It turns out our AOM with $f_0 = 79.16(37)$ MHz is within 2σ of the manufacturers value so in the future, fitting can be done without leaving this parameter free. Additionally we get a quality factor of

$$Q_1 = 4.87(17).$$

Furthermore, the change of the Bragg angle depending on the RF frequency is investigated. In Figure 7, Bragg angle θ_{B} is plotted against frequency f_{RF} . Again, the frequency is assumed to be perfect and only uncertainties from determining the angle matter.

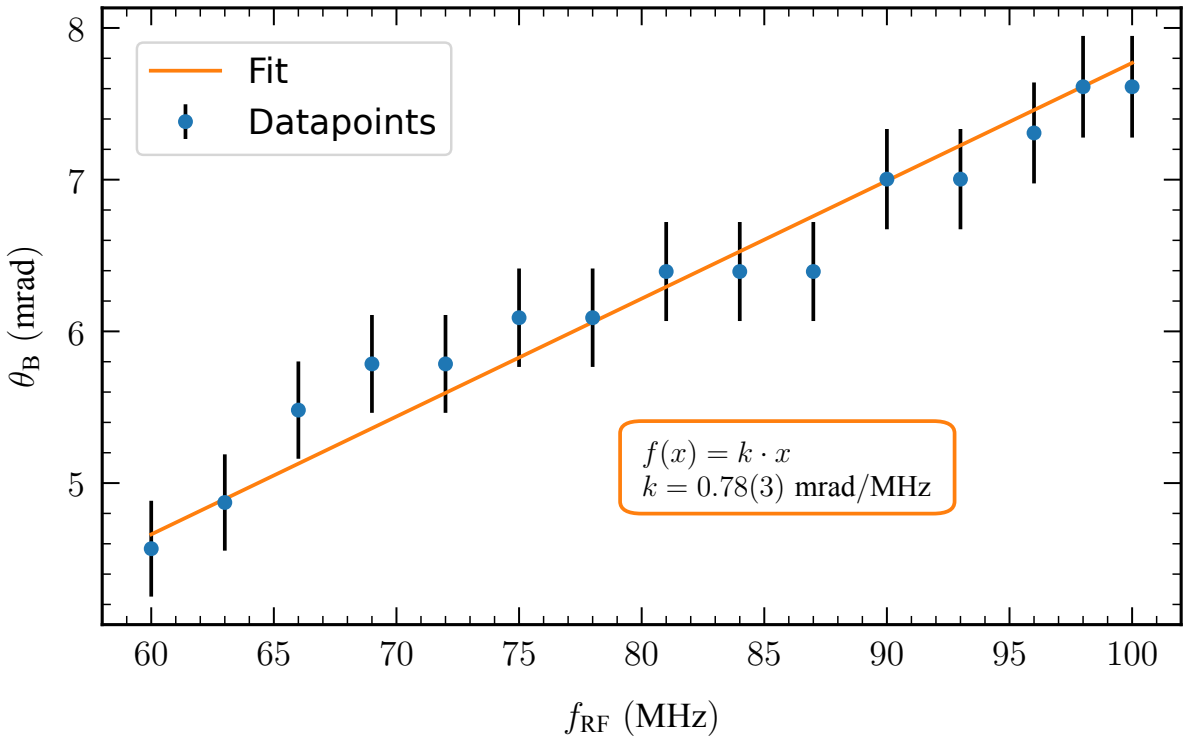

Figure 7: On the x-axis of this plot, frequency is plotted, whereas on the y-axis, the matching Bragg angle is shown. Furthermore, a linear fit is done through the data points.

As can be seen in the plot, the Bragg angle is increasing linearly with frequency. This is supported by a linear fit that describes the data points well. The discrete jumps in angle can be attributed to the millimeter ticks on the measuring tape, which were the smallest .

3.4 Measurement of the angle dependence and comparison of the quality factor

Now a different technique is used to determine the quality factor. This time, the angle of the AOM is adjusted around its optimum value by $\pm 1°$. We used the ticks on the micrometer screw of the rotating mount, which then have to be converted into angles. In figure Figure 8, the measured efficiency is plotted against the normalized angle difference Δ, which is defined as the deviation from the optimal angle, divided by the Bragg angle calculated in subsection 3.1. Equation (2) predicts again a $\sin(x)/x$ dependence, which was fitted and can also be seen in in Figure 8.

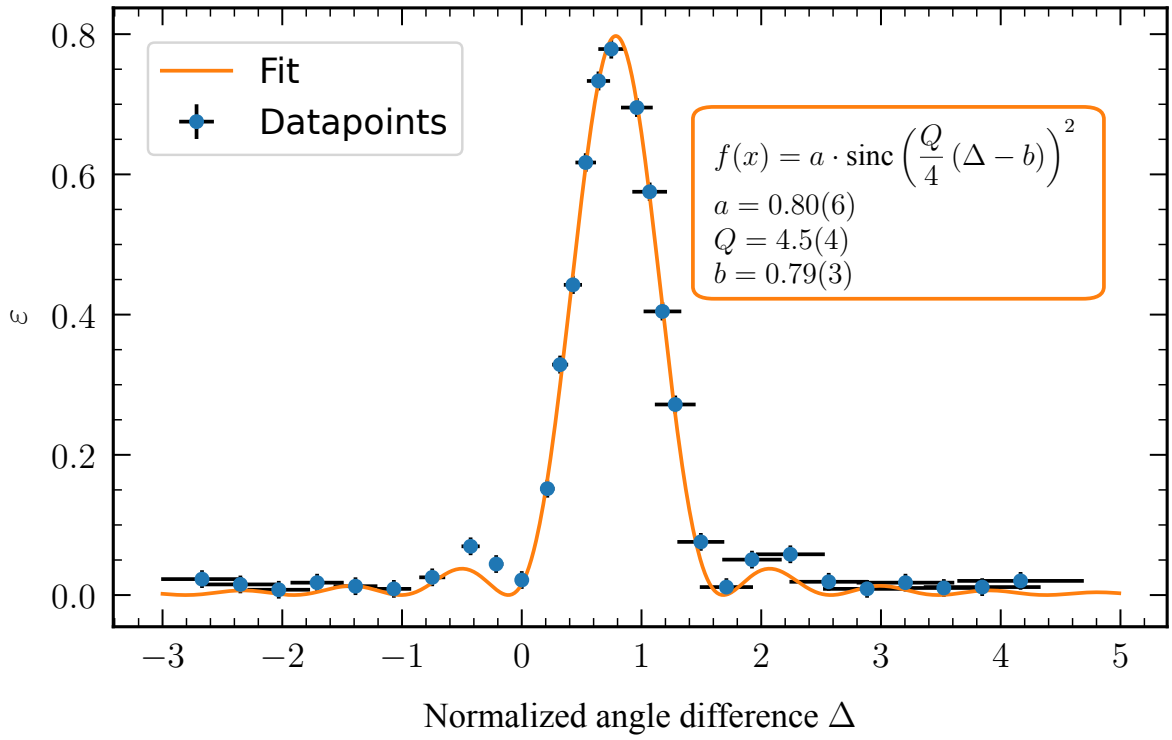

Figure 8: The efficiency is plotted depend in the normalized angle difference. A fit-function, described in the plot, is shown too.

We included the parameter b in the fit to catch systematic shifts due to the rotation mounts deadzone. From visual inspection we estimated it to be 5 ticks, the fit returns a value of $b = 7.37(4)$ ticks. Using the fit, we get a quality factor of

$$Q_2 = 4.5(4).$$

3.5 Measurement of the angular dependence of the maximum diffraction efficiency

In this part of the experiment, the RF frequency is varied from 60 MHz to 100 MHz, but in contrast to subsection 3.3, the Bragg angle is adjusted to maximise the efficiency. From these results we see how the maximum efficiency is behaving, depending on the RF frequency. In Figure 9, the maximum efficiency is plotted against the RF frequency.

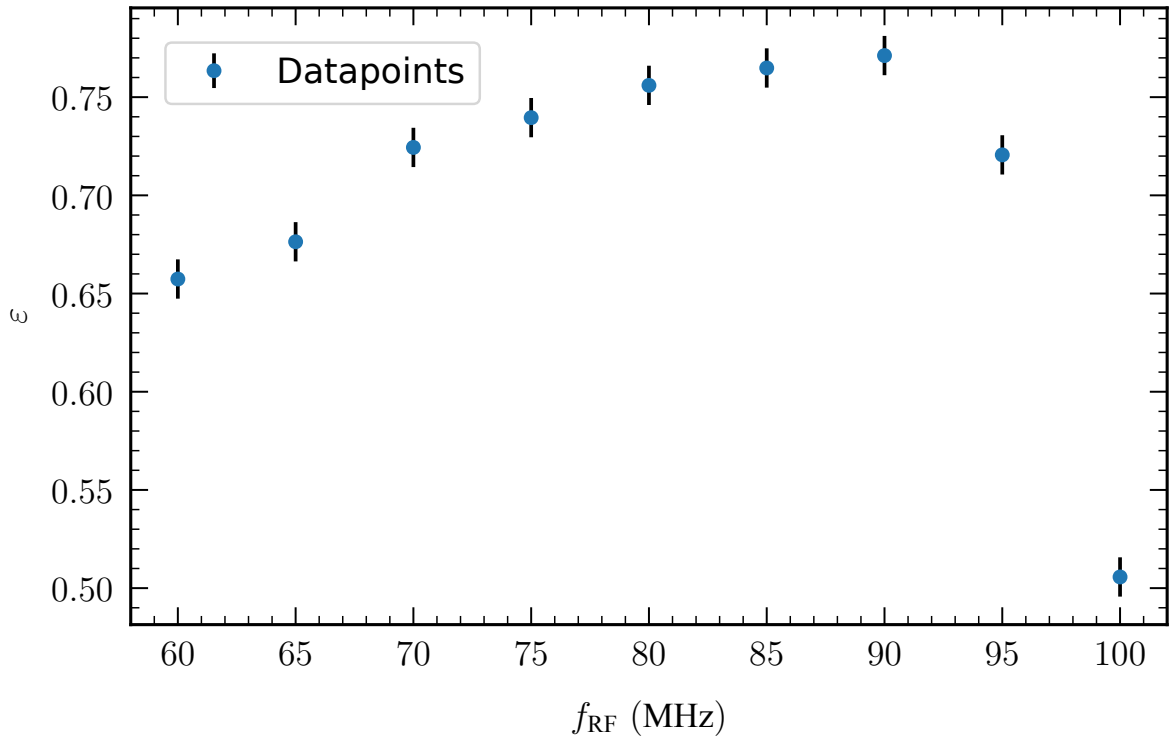

Figure 9: The maximum received efficiency, with optimised Bragg angle, is shown in dependence of the RF frequency f_{RF} .

4 Interpretation

In the first part of the experiment we determined the bragg angle to be $\theta_{\mathrm{B}} = 6.5(8)$ mrad. The datasheet of the AOM [3] tells us, that the Bragg angle for a laser with a wavelength of 633 nm equals 6 mrad. Comparing these two values, we see that our measured result is within 1σ of the literature value. However, our uncertainty is quite high and can be reduced by more accurately determining the distance between 0^{th} and 1^{st} order diffraction beams.

The reference value for the saturation power is 1 W. We measured $P_{\mathrm{sat}} = 1.21(3)$ W, which is significantly above the reference. This could have various reasons: a) the fit is not optimal with values lying systematically above/below the fitcurve and b) neglecting higher diffraction orders, that also receive power.

According to the data sheet, the insertion loss, is maximally 5 %. We measured 9.8(8) %, which means that significantly more energy is lost in the AOM than intended. This could be due to dirt/impurities on the inlet or outlet of the AOM.

By varying the RF frequency, we obtain a quality factor of $Q_1 = 4.87(17)$. The value of the quality factor by adjusting the angle, $Q_2 = 4.5(8)$, is around 8 % smaller, but with a much bigger uncertainty. These values are consisten with each other. Comparing the two methods, we conclude that varying the frequency is much more accurate than changing the angle, since the frequency can be assumed to be perfect, whilst manually changing the angle introduces statistical and, much more important, systematic errors, which have to be accounted for.

By analysing the relation between frequency and bragg angle, we conclude that the Bragg angle is increasing linearly with RF frequency.

In the last part of the experiment, we investigates whether we could retain maximum efficiency at off-resonant frequencies by readjusting the angle. According to our data, maximum efficiency can be achieved at around 90 MHz, although the efficiency is relatively constant in the range from 70 MHz to 90 MHz. Before and after, the efficiency decreases rapidly, especially at higher frequencies. This is probably due to internal geometric constraints acting like low/high pass filters for sound waves.

References

[1] Wikipedia contributors. *Bragg's law — Wikipedia, The Free Encyclopedia*. `https://en.wikipedia.org/w/index.php?title=Bragg%27s_law&oldid=1212831935`. [Online; accessed 15-March-2024]. 2024.

[2] . *Practical course experiment 08: Acousto-optical effect*. Universität Innsbruck, Innsbruck, AT: Institut für Experimentalphysik, 2024.

[3] A. Campi. *AOMO 3080-125, Part Nr: 97-01598-01*. Crystal Technology, Inc, 6.12.2002.

[4] . *Coaxial Amplifier(ZHL-1-2W+l)*. Brooklyn, NY ,USA: Mini-Circuits.

[5] H. Dr. *dBm - Voltage Chart*. Houston, TX 77036 — USA: Tecmag, Inc.

[6] *METRIC PRECISION ROTATION PLATFORM,PR01/M*. w w w . t h o r l a b s . c o m, 15.4.2013.

Erklärung

Hiermit versichern wir, dass der vorliegende Bericht selbständig verfasst wurde und alle notwendigen Quellen und Referenzen angegeben sind.

March 19, 2024

Alexander Helbok — Date

March 19, 2024

Jakob Hugo Höck — Date

March 19, 2024

Max Koppelstätter — Date